JOURNAL OF ENZYME INHIBITION AND MEDICINAL CHEMISTRY
2023, VOL. 38, NO. 1, 2121821
https://doi.org/10.1080/14756366.2022.2121821

Taylor & Francis
Taylor & Francis Group

RESEARCH PAPER

OPEN ACCESS Check for updates

Combining nano-differential scanning fluorimetry and microscale thermophoresis to investigate VDAC1 interaction with small molecules

Hubert Gorny[a], Angélique Mularoni[a], Jean-Guy Delcros[a], Céline Freton[b], Jordane Preto[a] and Isabelle Krimm[a]

[a]Centre de Recherche en Cancérologie de Lyon, Université Claude Bernard Lyon 1, INSERM 1052, CNRS 5286, Centre Léon Bérard, Lyon, France; [b]Molecular Microbiology and Structural Biochemistry, UMR 5086, Université de Lyon, CNRS, Lyon, France

ABSTRACT

The mitochondrial voltage-dependent anion channel 1 (VDAC1) plays a central role in metabolism and apoptosis, which makes it a promising therapeutic target. Nevertheless, molecular mechanisms governing VDAC1 functioning remain unclear. Small-molecule ligands specifically interacting with the channel provide an attractive way of exploring its structure-function relationships and can possibly be used as founding stones for future drug-candidates. While around 30 VDAC1 ligands have been identified over the years, various techniques have been used by research teams, making a fair and direct comparison between compounds impossible. To tackle this issue, we performed ligand-binding assays on a representative set of seventeen known VDAC1 ligands using nano-differential scanning fluorimetry and microscale thermophoresis. While all the compounds have been confirmed as VDAC1 ligands by at least one method, combining both technologies lead to the selection of four molecules (cannabidiol, curcumin, DIDS and VBIT4) as chemical starting points for future design of VDAC1 selective ligands.

ARTICLE HISTORY
Received 1 August 2022
Revised 1 September 2022
Accepted 1 September 2022

KEYWORDS
VDAC1; microscale thermophoresis; nano-differential scanning fluorimetry

Introduction

The voltage-dependent anion channel 1 (VDAC1) is the most abundant protein of the outer mitochondrial membrane (OMM). VDAC1 is responsible of approximatively 90% of the exchanges between the mitochondrion and the cytoplasm regulating the transport of most ions and metabolites of molecular weight less than 5 kDa[1–3]. In addition, the channel is considered a hub protein interacting with many partners involved in the mitochondrial function including apoptosis[4–6]. In response to a pro-apoptotic signal, VDAC1 was shown to homo-oligomerize forming a large pore that enables the release of apoptogenic factors from the mitochondrial intermembrane space (IMS) to the cytosol[5,7,8]. Apoptogenic factors include the apoptosis inducing factor (AIF), Smac/DIABLO and the cytochrome C, leading to caspase activation and subsequent cell death. The above factors can also be released via large hetero-oligomers made of VDAC1 and of the pro-apoptotic protein Bax from the Bcl-2 family, resulting in the same apoptotic effects[9]. The pro-apoptotic activity of VDAC1 can be regulated through its interaction with anti-apoptotic partners including members of the Bcl-2 family (BcL-XL, Bcl-2)[10] as well as Hexokinases I and II (HKI and HK2) that prevent the formation of large-pore oligomers involving VDAC1[11]. Efforts are currently being made to provide insights into the structure of VDAC1 complexes including homo-[7], hetero-oligomers and the HK-VDAC1 complex[12,13] although no experimental structure of these complexes has yet been obtained. As a result, related mechanisms and their relationships to channel function remain largely misunderstood.

At the structural level, VDAC1 is made of a 19-strand β-barrel pore and an α-helical N-terminal domain composed of the first 25 residues[14–16]. In the absence of a transmembrane (TM) voltage, the channel is stable in its open state transporting most ions and small metabolites with a preference for anions (Figure 1). At high TM voltage, i.e., below -30 mV or above $+30$ mV, typically, VDAC1 can switch from its open state to multiple closed states[17]. Closed states are characterised by a reduced conductance for ions, are impermeable to large metabolites and show a preference for cations[18]. Recent advances have suggested that the N-terminal domain was a critical component to promote channel closure[19,20] and interaction with protein partners[10,21]. However, molecular mechanisms governing the functioning of VDAC1 as well as the impact of these mechanisms at the cellular level have yet to be described. On this basis, small-molecule ligands constitute valuable tools as they can be utilised as molecular probes to modulate channel activity and dissect its mechanisms[22]. In this regard, highly selective and affine VDAC1 ligands are required to investigate VDAC1 functions in cells. This is a challenging task as VDAC1 is often regarded as undruggable due to the absence of a well-defined binding site[23].

Most small molecules that have been reported to directly interact with VDAC1 correspond to standard compounds like aspirin, curcumin, itraconazole or ruthenium red (RuR)[24–27]. These ligands are well-known to interact with various targets unrelated to VDAC1 making them non-specific to the channel. Among all reported ligands, only SC18, identified by Heslop et al.[28] at the time of this study writing, and VBIT4 and its derivatives (Akos022, VBIT3 and VBIT12) have been developed to act specifically on

CONTACT Jordane Preto jordane.preto@univ-lyon1.fr; Isabelle Krimm isabelle.krimm@univ-lyon1.fr Centre de Recherche en Cancérologie de Lyon, Université Claude Bernard Lyon 1, INSERM 1052, CNRS 5286, Centre Léon Bérard, Lyon, France

Supplemental data for this article is available online at https://doi.org/10.1080/14756366.2022.2121821.

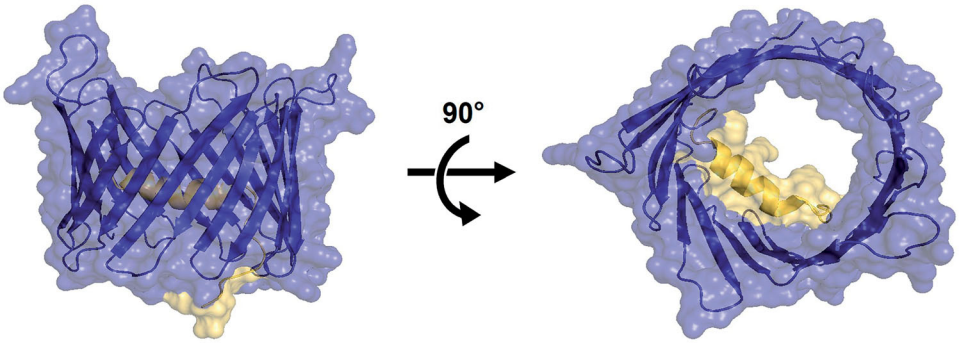

Figure 1. Structure of the open state of hVDAC1 in LDAO micelles (PDBID:2JK4)[15]. Left: side (membrane) view. Right: top (cytoplasm) view. The barrel pore is coloured in blue and the alpha helix in yellow.

VDAC[29]. VBIT-4 activity as VDAC1 interacting molecule inhibiting apoptosis was demonstrated for several diseases as Type 2 diabetes[30], lupus[31], and Colitis[32], pointing to VBIT-4 as an emerging drug candidate. This highlights the clinical importance of developing new VDAC1 ligands.

Multiple techniques have been employed to demonstrate the direct interaction of ligands with the channel including conductance measurement in Planar Lipid Bilayer (PLB)[24], affinity chromatography[33], Microscale Thermophoresis (MST)[34] and Photoaffinity Labelling[35], to name but a few, thereby preventing qualitative or quantitative comparison between ligands. Although dissociation constants (K_d) were measured (mostly by MST) for a few compounds including ATP[36], cannabidiol[34], erastin[37] and NADH[38], experimental setups involved different VDAC isoforms (VDAC1, VDAC2 and VDAC3), source organisms and/or lipid environment and/or detergent which can have important consequences on reported K_d values. In the quest of finding specific small-molecule ligands that can serve as molecular probes to explore VDAC1 mechanisms, we propose a single experimental protocol which combines MST and nano-differential scanning fluorimetry (NanoDSF) to re-evaluate a representative set of seventeen presumed VDAC1 ligands. Specifically, all the tested molecules were confirmed as ligands by a least one method whereas eleven were validated by both techniques. In addition, dissociation constants were estimated for six out of the seventeen compounds. These results allowed a fair comparison of different classes of VDAC1 ligands in order to prioritise them for future experiments.

Materials and methods

Materials

E. coli BL21 were purchased from Invitrogen. Plasmid pET-21A was purchased from Novagen. pDNR-LIR-hVDAC was purchased from Dharmacon. Ampicillin, IPTG, Triton 100X, Guanidine hydrochloride, Acrylamide: Bisacrylamide 37.5:1, SDS 10%, Temed, APS, TGS 10X, NH_4Cl and $CaCl_2$ were purchased from Euromedex. NaCl, NaH_2PO_4, K_2HPO_4, KH_2PO_4, glucose, LB-broth, Tris-HCl, NADH, propofol, quinidine, ubiquinone 0, Laemli 6X, β-mercaptoethanol, PBS, Na_2HPO_4, K_2SO_4 and metformin were purchased from ThermoFisher. Aspirin, catechin, curcumin, DCCD, DPC, emodin, fluoxetine, and $MnCl_2$ were purchased from Fluorochem. Imidazole, DIDS, DMSO, ReadyBlue Protein Gel stain, EDTA, $MgCl_2$, $CoCl_2$, H_2BO_3, acetone and ethanol were purchased from Sigma-Aldrich. $FeSO_4$ and $ZnSo_4$ were purchased from Biobasic. $CuCl_2$ and Mo_7O_{24} were purchased from Roth. $^{15}NH_4Cl$, D_2O and deuterated glucose were purchased from Innova-Chem. LDAO was purchased from CliniSciences. Itraconazole was purchased from Cayman Chemical company. VBIT4 was purchased from Aobious. Cannabidiol was purchased from Carbosynth. Olesoxime was obtained from in-house chemical library.

Preparation of His6-tagged human VDAC1

hVDAC1 cDNA was subcloned into pET21A from pDNR-LIR-hVDAC. hVDAC1 was produced in BL21 *E. coli* transformed with a pET-21a plasmid (supplemental Figure S1A) containing the hVDAC1-coding sequence and purified as described in[39]. The protein was extracted from inclusion bodies in Guanidium containing buffer. The denatured protein was purified by affinity chromatography on a HisTalon superflow Cartridge column (Takara bio-Company) followed by size-exclusion chromatography (SEC; HiLoad 16/600 Superdex 200 pg, Cytiva). VDAC1 refolding was performed by dropwise dilution into a buffer supplemented with 1% LDAO[39]. The protein was purified by cation exchange chromatography (HiLoad 16/10 SP Sepharose HP; Cytiva) followed by a SEC. Protein purity was verified by SDS-PAGE (supplemental Figure S1B) and Coomassie staining. Proper folding of the protein was confirmed by ^{1}H-^{15}N TROSY-HSQC performed with 90 µM of perdeuterated hVDAC1 in a 5 mm tube on a 950 MHz Bruker spectrometer equipped with a cryogenically cooled probe (supplemental Figure S2).

NanoDSF analysis

hVDAC1 (50 µg/mL) was incubated 20 min with each compound in the experimental buffer (PBS, pH 7.2 with 0.1% LDAO) containing either 0% or 5% DMSO depending on compound solubility. Next, samples were loaded into NanoDSF Standard-grade capillaries and transferred into a Prometheus NT.48 NanoDSF device (NanoTemper Technologies). Thermal unfolding was detected during heating in a linear thermal ramp (2 °C/min; 30–80 °C) with an excitation power of 20%. Unfolding transition points were determined from changes in the emission wavelengths of tryptophan fluorescence at 330 nm and 350 nm, respectively, and from the ratio 350/330 nm. Experiments were conducted in triplicates and data were analysed using the Prometheus PR stability analysis software.

MST analysis

Purified hVDAC1 was fluorescently labelled using NanoTemper Protein labelling kit RED-NHS 2nd generation (L011, NanoTemper Technologies) or labelling kit BLUE-NHS (L003) depending on ligand fluorescence according to manufacturer instructions. hVDAC1

Table 1. List of selected compounds including experimental techniques used to show direct interaction as well as observed effect(s) on VDAC1 and corresponding references.

Compound	Technique(s) showing direct interaction	Effect(s) on activity	Reference
Aspirin	PLB	Reduces conductance Induces VDAC-HK II detachment	24
Cannabidiol	PLB, MST	Reduces conductance Increases mitochondrial Ca^{2+}	34
Catechin	Affinity chromatography		33
Curcumin	PLB	Reduces conductance by promoting closed state(s)	25
DCCD	PLB, NMR [^{14}C] DCCD-labelled VDAC1	Reduces conductance Inhibits HK-VDAC1 binding	44,46,47,48
DIDS	PLB, MST	Reduces conductance by complete closure of the channel Inhibits oligomerization	48,49
DPC	PLB, MST	Reduces conductance Prevents oligomerization	49
Emodin	Affinity chromatography		33
Fluoxetine	PLB	Reduces conductance Prevents Cyto C release	50,51
Itraconazole	PLB, Photoaffinity labelling MST	Reduces conductance	35,26
Metformin	PLB, MST	Reduces conductance No binding observed by MST	30
NADH	PLB, NMR	Affects gating without reducing the conductance Sterically closes the channel	38,52,14
Olesoxime	PLB	Reduces conductance	53
Propofol	PLB	Promotes closure when a negative voltage is applied No effects on open state conductance	54
Quinidine	PLB	Reduces conductance by steric blockage	55
Ubiquinone 0	Photoaffinity labelling	Induces over-expression of VDAC	56,57
VBIT4	PLB, MST	Reduces conductance Inhibits oligomerization Inhibits HK detachment	29

Structures of compounds are shown in supplementary Figure S3.

(100 nM) was incubated 20 min with each compound in the dark at room temperature at the highest soluble ligand concentration (binding check experiment) or at 16 different concentrations obtained by serial dilution starting from the highest soluble concentration (dose-response experiment). Samples were loaded into glass capillaries (Monolith NT Capillaries), and thermophoresis analysis was performed using a Nano-Temper Monolith NT.115 apparatus. (LED power 20%, IR laser power 20%). Signal quality was monitored by the NanoTemper Monolith device to detect possible ligand auto-fluorescence, precipitation, aggregation, or ligand-induced changes in the photobleaching rate. Experiments were conducted as triplicates and treated with the MO.Affinity Analysis software (Nano-Temper).

Results

Dataset

About 13 ligands of VDAC, excluding analogues, have been described in the literature so far. One of the most recent and complete review on VDAC ligands[40] was used for the selection of the compounds tested in the present work. A high structural heterogeneity in the selected set was a primordial criterion. Fragment-size molecules (aspirin, propofol) to much more complex molecules (itraconazole) were picked by keeping, at most, two compounds of the same family. The selected molecules also included ligands expected to bind inside the pore region (aspirin, curcumin, emodin …)[33,41] and ligands most likely binding to the outer, i.e., lipid-facing, part of the channel (propofol, olesoxime)[42,43]. Importantly, DCCD was shown to covalently bind to VDAC[44]. As reported for other channels, DIDS might as well bind covalently to VDAC[45]. The seventeen compounds investigated in the present study are listed in Table 1 where we also specified the original experimental technique(s) used to demonstrate direct interaction and the reported effect(s) on channel activity.

VDAC1 samples

Recombinant human VDAC1 (hVDAC1) samples were produced according to the protocol published by Silver et Eddy[39]. The proper refolding of the protein was assessed by ^{1}H-^{15}N TROSY-HSQC NMR experiment. The NMR spectrum (supplemental Figure S2) was comparable to those published[14,15], which confirmed the correct refolding of the protein.

NanoDSF measurements

NanoDSF is a label-free thermal-shift-assay (TSA) technique used to study protein denaturation as a function of the temperature. NanoDSF provides indications on protein stability and enables to determine the binding ability of small molecules for targets of interest. The technique is based on the estimation of the melting temperature (T_m) of the protein by monitoring the intrinsic fluorescence of tryptophan residues. When excited at wavelengths around 280 nm, Tryptophans emit fluorescence as a peak around 330 nm when they are embedded in hydrophobic areas of the folded state, while they emit at 350 nm when they become exposed to the hydrophilic solvent during unfolding[58]. hVDAC1 structure includes four tryptophans (W64, W75, W149 and W210) facing the lipid membrane. Varying the fluorescence intensity ratio (F350 nm/F330 nm) as a function of the temperature resulted in a S-shaped transition from the folded to the denatured state, usually referred to as redshift, which is the most common transition observed by NanoDSF[59]. The melting temperature was first evaluated on hVDAC1 alone in the absence of ligands (Figure 2). Average T_m values were determined at $57.6 \pm 0.05\,^{\circ}C$ and $56 \pm 0.07\,^{\circ}C$, at 0% and 5% DMSO, respectively, which is comparable to the T_m measured by TSA on CPM-labelled mVDAC1, i.e., $T_m = 55.8 \pm 0.6\,^{\circ}C$ in the absence of DMSO[60]. Next, T_m values were determined in the presence of the seventeen selected compounds and compared to the T_m of hVDAC1 alone at 0%, or 5% DMSO when the compound was not soluble at 0% DMSO. The thermal shift (ΔT_m) was considered significant when it exceeded three times the standard deviation of the T_m in the absence of a ligand ($\pm$ 0.22 °C). In this case, the compound was assumed to be a genuine ligand of hVDAC1.

As shown in Figure 3, 13 out of the seventeen compounds have been confirmed as VDAC1 ligands as they induced a significant shift in the T_m. Among them, six molecules (aspirin,

cannabidiol, catechin, DCCD, fluoxetine and propofol) were found to increase the T_m. In contrast, seven molecules (curcumin, DIDS, DPC, olesoxime, quinidine, ubiquinone, VBIT4) induced a negative T_m shift. The four remaining compounds (emodin, itraconazole, NADH and metformin) have not been confirmed as VDAC1 ligands by NanoDSF in our experimental conditions.

MST measurements

MST enables to track temperature-induced changes in the fluorescence of a fluorochrome-tagged protein. When a ligand binds to a target, its MST signal is modified in a ligand concentration-dependent manner[61]. Therefore, the MST technique can either be used as a single-dose assay (i.e., at fixed ligand concentration) to determine the binding ability of a compound or at multiple concentrations in order to build dose-response curves from which the dissociation constant can be estimated. In this study, both approaches were applied. The seventeen compounds were first tested by single-dose assay referred to as binding check (Figure 4). A significant modification in the MST signal compared to the reference signal (protein alone) was observed for every compound except for ubiquinone. No information about the binding ability of catechin was obtained as auto-fluorescence, photobleaching rate modification and aggregation of the protein were systematically observed upon addition of this compound.

The fifteen ligands confirmed by single-dose assay were further investigated to determine their dissociation constant (K_d). Transition of the signal from the saturated-protein state (high ligand concentration) to the free-protein state (low ligand concentration) was monitored to determine the K_d (Figure 5). Overall, dissociation constants were successfully determined for six compounds including DIDS (K_d = 0.5 µM), VBIT4 (K_d = 3 µM), itraconazole (K_d = 5 µM), cannabidiol (K_d = 6 µM), curcumin (K_d = 6 µM) and emodin (K_d = 10 µM). As mentioned above, DIDS is likely to

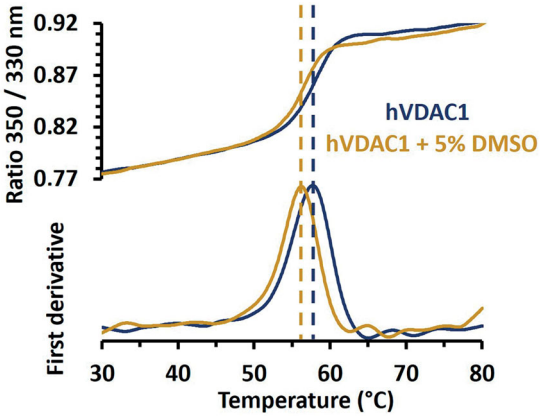

Figure 2. Thermal stability of hVDAC1 in LDAO micelles determined by NanoDSF in presence or absence of 5% DMSO. The S-shaped transition of the ratio of tryptophan fluorescence at 350 and 330 nm is displayed in the top figure while corresponding first derivatives are shown in the bottom figure. Inflection points, which correspond to the T_m, are indicated by dashed lines. T_m values were 57.60 ± 0.05 °C and 56.00 ± 0.07 °C in the absence or in the presence of 5% DMSO, respectively. Standard deviations were obtained by performing triplicates of each experiment.

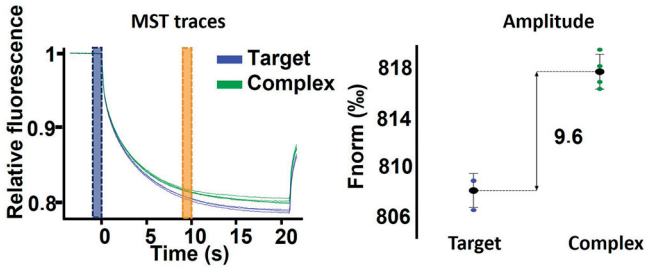

Figure 4. MST binding check performed on 100 nM hVDAC1 with (green), or without (blue) 250 µM VBIT4.

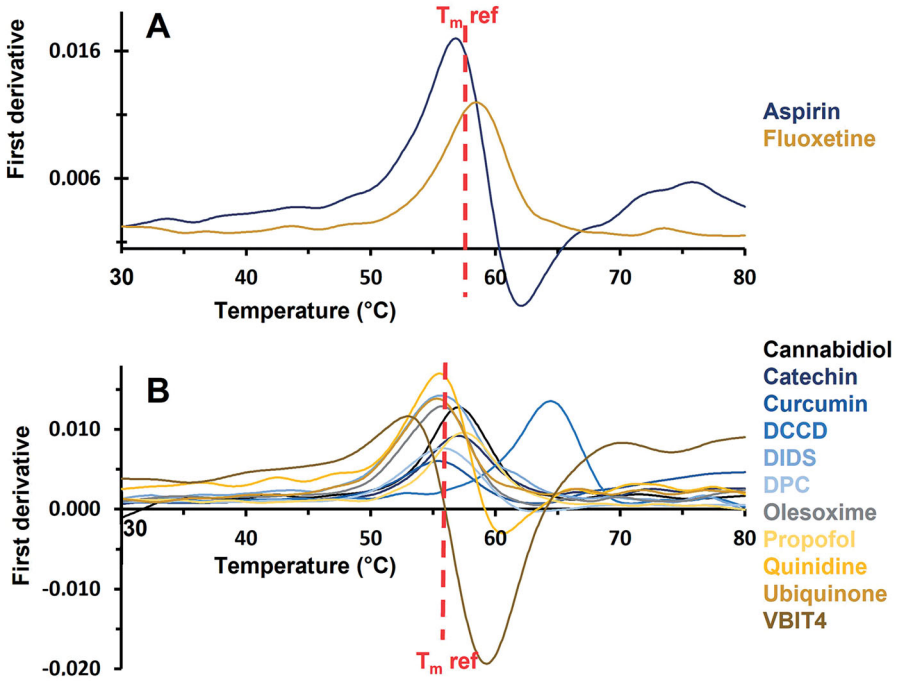

Figure 3. First derivative of the 350/330 nm ratio obtained from NanoDSF as a function of the temperature. Only compounds displaying a significant T_m shift are shown. (A) Compounds solubilised in buffer. (B) Compounds solubilised in DMSO. Reference T_m, obtained for hVDAC1 (in absence (A) or in presence of 5% DMSO (B)) is indicated.

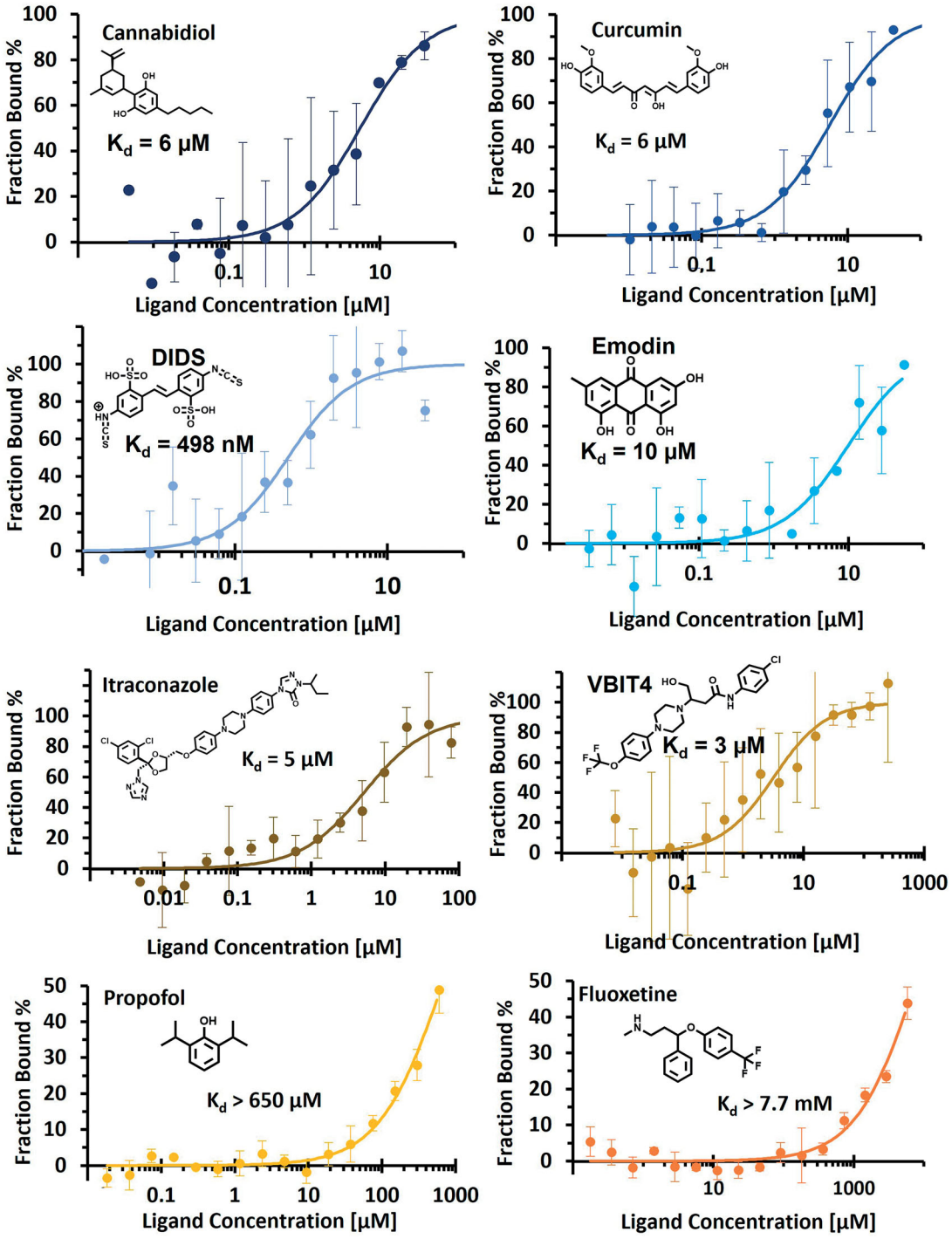

Figure 5. MST dose-response curve of the eight compounds displaying precise or minimum K_d values (cannabidiol, curcumin, DIDS, emodin, itraconazole, VBIT4, propofol and fluoxetine). Error bars show standard deviation obtained from three replicas of the same measurement.

interact covalently with VDAC1. Therefore, the measured K_d must be carefully considered. Evaluation of the K_d was not possible for propofol and fluoxetine since the saturation plateau could not be reached (K_d > 650 µM for propofol and K_d > 7.7 mM for fluoxetine). The dissociation constant of six compounds (aspirin, DPC, metformin, NADH, olesoxime, and quinidine) could not be determined despite being validated by binding check. Indeed, no transition from the unbound to the bound state was observed for these ligands, which was likely due to a poor ligand affinity or a too weak modification of the fluorescence resulting in a too small signal amplitude. In contrast with a previous study[49], no proper dose-response data were obtained for DPC preventing the evaluation of the K_d. Similarly, we could not obtain dose-response data for DCCD which, in this case, may be related to the ability of the compound to form covalent bonds with proteins[44,46].

K_d values determined for cannabidiol (6 µM) and VBIT4 (3 µM) were in good agreement with published data, i.e., 11 µM for cannabidiol[34] and 53 µM for VBIT4[29], while a significant difference was found for itraconazole (K_d = 5 vs 120 µM in[26]). Finally, the present work is reporting for the first time the affinity of curcumin and emodin for VDAC1, with K_d values of 6 µM and 10 µM, respectively.

A summary of the results obtained with both techniques (NanoDSF and MST) is provided in Table 2. Every tested

Table 2. Results obtained by NanoDSF and MST including T_m shift, MST binding check and dissociation constant evaluated for each tested compounds and published affinity if available. A thermal shift was considered significant when its variation exceeded ± 0.22 °C. (N.D., not determined, when experiments were not performed due to inconclusive binding check assay; N.A., not available, when experiments were performed but were inconclusive). hVDAC1 = human recombinant VDAC1 and rVDAC1 = VDAC1 extracted from rat.

Compound	ΔT_m °C	MST Binding Check	K_d (μM)	Published K_d (μM)
Aspirin	+1.01	Positive	N.A.	
Cannabidiol	+0.94	Positive	6 ± 2	11.2 [rVDAC1]
Catechin	+0.91	N.A.	N.D.	
Curcumin	−0.76	Positive	6 ± 1	
DCCD	+8.19	Positive	N.A.	
DIDS	−0.53	Positive	0.5 ± 0.2	70 [rVDAC1]
DPC	−0.45	Positive	N.A.	150 [rVDAC1]
Emodin	−0.21	Positive	10 ± 5	
Fluoxetine	+0.81	Positive	>7 700	
Itraconazole	−0.22	Positive	5 ± 2	120 [rVDAC1]
Metformin	+0.12	Positive	N.A.	
NADH	+0.18	Positive	N.A.	9000 (hVDAC1)
Olesoxime	−0.56	Positive	N.A.	
Propofol	+1.31	Positive	>650	
Quinidine	−0.82	Positive	N.A.	
Ubiquinone 0	−0.94	Negative	N.D.	
VBIT4	−3.51	Positive	3 ± 1	53 [hVDAC1]

compound was confirmed as ligand by at least one technique and eleven out of seventeen were confirmed with both single dose assays. Four molecules did not induce a significant T_m shift in NanoDSF but were confirmed as ligands by MST binding check. Overall, only two ligands were not confirmed by binding check (ubiquinone and catechin) whereas they induced a significant T_m shift in NanoDSF. As no ligands were simultaneously unvalidated by both methods, this suggests that the combination of NanoDSF and MST might provide an efficient way to reduce false negatives in low- or medium-throughput screening campaigns.

Discussion

Although VDAC1 is central to many physiological processes and involved in various diseases, its pharmacological potential remains uncertain[23,62]. To address this issue, small-molecule ligands provide suitable research tools in order to understand channel mechanisms[22]. So far, around thirty compounds have been described as VDAC1 ligands[40] while dissociation constants have been measured for a few of them. Many techniques, conditions and protein isoforms have been used to characterise these compounds which makes a fair comparison between them difficult. In the present study, we used a single experimental protocol based on scanning fluorimetry and microscale thermophoresis to re-evaluate a representative panel of seventeen presumed VDAC1 ligands. For all the compounds, the same experimental conditions and a single recombinant human VDAC1 sample were employed thereby providing a common basis to analyse and prioritise molecules.

In general, a correct agreement was observed between NanoDSF and MST techniques (11 out 16 compounds were confirmed as ligands by both single dose assay; catechin could not be studied by MST). However, for emodin and itraconazole, binding was shown using the MST technique, while no significant changes in T_m was observed using NanoDSF. As reported in[63], such discrepancies may be related to the characteristics of each approach. In particular, the binding of a compound does not systematically modify the stability of the protein, and therefore would not induce a significant shift in the T_m.

Besides synthetic ligands, the combination of MST and NanoDSF to analyse the binding of physiological VDAC1 regulatory molecules such as ATP, glutamate or Ca2+ would deserve further investigation. This should also provide insights into the effect of these natural regulatory molecules on the binding of synthetic VDAC1 ligands.

Among all the ΔT_m measured by NanoDSF, DCCD displayed the largest value (+8.19 °C) which is expected to be due to its ability to covalently bind to carboxyl residues located inside hydrophobic pockets[64]. In the case of VDAC1, DCCD was shown to interact with the lipid-facing E73 residue using [^{14}C]-DCCD labelling[44]. This was later confirmed by protein-observed NMR experiments[46].

Overall, a stabilisation of the channel was observed (positive thermal shift) for six of the ligands whereas seven of them induced a destabilisation (negative thermal shift). The presence of both negative and positive induced thermal shifts as well as the absence of a common chemical skeleton between ligands may be indicative of multiple binding sites inside VDAC1 as suggested in[65]. Remarkably, no apparent correlation between the molecular properties of the thirteen ligands (molecular weight, logP, number of H-donors and acceptors, number of aromatic rings and pK_a) and their impact on the stabilisation of the protein was found, which also supports the idea of different binding areas within the channel.

In total, four compounds, i.e., cannabidiol, curcumin, DIDS and VBIT4, were confirmed by both NanoDSF and MST while displaying a reasonably low K_d value ($K_d < 10$ μM), and therefore constitute promising ligands to further investigate VDAC1 mechanisms or druggability.

Structural studies, e.g., based on X-ray crystallography or NMR, may help confirm ligand binding sites as well as estimate the impact of these compounds on VDAC1 stabilisation. As positive (cannabidiol) and negative (curcumin, DIDS and VBIT4) T_m shifts were observed, both destabilisation and stabilisation of the channel could be explored *a priori*. Finally, we believe that such compounds can serve as starting points for chemical modification to design innovative ligands with higher specificity and affinity, that could be used later on to investigate the therapeutic potential of VDAC1 ligands in various diseases.

Conclusion

In this paper, 17 compounds known as VDAC1 ligands in the literature were studied by NanoDSF and MST. All the ligands were validated by at least one technique and eleven were confirmed by both, suggesting that this approach is promising for the study of other reported ligands and the identification of novel VDAC1 binders. Among the compounds validated by both methods, four of them (cannabidiol, curcumin, DIDS and VBIT4) displayed a reasonably low K_d value, which makes them promising chemical starting points to design molecular probes for further exploration of VDAC1 functions.

Disclosure statement

No potential conflict of interest was reported by the author(s).

Funding

This work was supported by institutional grants from the Centre National de la Recherche Scientifique (CNRS), the Centre Leon

Bérard, Institut Convergence PLAsCAN [ANR-17-CONV-0002] and the Ligue Contre le Cancer (Comité de Haute-Savoie).

References

1. Magrì A, Di Rosa MC, Orlandi I, et al. Deletion of Voltage-Dependent Anion Channel 1 knocks mitochondria down triggering metabolic rewiring in yeast. Cell Mol Life Sci. 2020;77:3195–213.
2. Rosencrans WM, Rajendran M, Bezrukov SM, Rostovtseva TK. VDAC regulation of mitochondrial calcium flux: from channel biophysics to disease. Cell Calcium 2021;94:102356.
3. Colombini M. VDAC: the channel at the interface between mitochondria and the cytosol. Mol Cell Biochem 2004;256: 107–15.
4. Shoshan-Barmatz V, Maldonado EN, Krelin Y. VDAC1 at the crossroads of cell metabolism, apoptosis and cell stress. Cell Stress 2017;1:11–36.
5. Keinan N, Tyomkin D, Shoshan-Barmatz V. Oligomerization of the mitochondrial protein voltage-dependent anion channel is coupled to the induction of apoptosis. Mol Cell Biol 2010;30:5698–709.
6. Shoshan-Barmatz V, De Pinto V, Zweckstetter M, et al. VDAC, a multi-functional mitochondrial protein regulating cell life and death. Mol Aspects Med 2010;31:227–85.
7. Hosaka T, Okazaki M, Kimura-Someya T, et al. Crystal structural characterization reveals novel oligomeric interactions of human voltage-dependent anion channel 1: Novel Oligomeric Structure of Human VDAC1. Protein Sci 2017;26: 1749–58.
8. Huang L, Han J, Ben-Hail D, et al. A new fungal diterpene induces VDAC1-dependent apoptosis in Bax/Bak-deficient cells. J Biol Chem 2015;290:23563–78.
9. Tajeddine N, Galluzzi L, Kepp O, et al. Hierarchical involvement of Bak, VDAC1 and Bax in cisplatin-induced cell death. Oncogene 2008;27:4221–32.
10. Arbel N, Ben-Hail D, Shoshan-Barmatz V. Mediation of the antiapoptotic activity of Bcl-xL protein upon interaction with VDAC1 protein. J Biol Chem 2012;287:23152–61.
11. Azoulay-Zohar H, Israelson A, Abu-Hamad S, Shoshan-Barmatz V. In self-defence: hexokinase promotes voltage-dependent anion channel closure and prevents mitochondria-mediated apoptotic cell death. Biochem J 2004;377: 347–55.
12. Rosano C. Molecular model of hexokinase binding to the outer mitochondrial membrane porin (VDAC1): implication for the design of new cancer therapies. Mitochondrion 2011; 11:513–9.
13. Geula S, Ben-Hail D, Shoshan-Barmatz V. Structure-based analysis of VDAC1: N-terminus location, translocation, channel gating and association with anti-apoptotic proteins. Biochem J 2012;444:475–85.
14. Hiller S, Garces RG, Malia TJ, et al. Solution structure of the integral human membrane protein VDAC-1 in detergent micelles. Science 2008;321:1206–10.
15. Bayrhuber M, Meins T, Habeck M, et al. Structure of the human voltage-dependent anion channel. Proc Natl Acad Sci 2008;105:15370–5.
16. Ujwal R, Cascio D, Colletier J-P, et al. The crystal structure of mouse VDAC1 at 2.3 A resolution reveals mechanistic insights into metabolite gating. Proc Natl Acad Sci 2008;105: 17742–7.
17. Najbauer EE, Becker S, Giller K, et al. Structure, gating and interactions of the voltage-dependent anion channel. Eur Biophys J 2021;50:159–72.
18. Colombini M. Voltage gating in the mitochondrial channel, VDAC. J Membr Biol 1989;111:103–11.
19. Preto J, Gorny H, Krimm I. A deep dive into VDAC1 conformational diversity using all-atom simulations provides new insights into the structural origin of the closed states. Int J Mol Sci 2022;23:1175.
20. Mertins B, Psakis G, Grosse W, et al. Flexibility of the N-terminal mVDAC1 segment controls the channel's gating behavior zhang Z, editor. PLoS ONE 2012;7:e47938.
21. Abu-Hamad S, Arbel N, Calo D, et al. The VDAC1 N-terminus is essential both for apoptosis and the protective effect of anti-apoptotic proteins. J Cell Sci 2009;122:1906–16.
22. Arrowsmith CH, Audia JE, Austin C, et al. The promise and peril of chemical probes. Nat Chem Biol 2015;11:536–41.
23. Reina S, De Pinto V. Anti-cancer compounds targeted to VDAC: potential and perspectives. Curr Med Chem 2017;24: 4447–69.
24. Tewari D, Majumdar D, Vallabhaneni S, Bera AK. Aspirin induces cell death by directly modulating mitochondrial voltage-dependent anion channel (VDAC). Sci Rep 2017;7: 45184.
25. Tewari D, Ahmed T, Chirasani VR, et al. Modulation of the mitochondrial voltage dependent anion channel (VDAC) by curcumin. Biochim Biophys Acta (BBA) - Biomembr 2015; 1848:151–8.
26. Arif T, Krelin Y, Nakdimon I, et al. VDAC1 is a molecular target in glioblastoma, with its depletion leading to reprogrammed metabolism and reversed oncogenic properties. Neuro-Oncology 2017;19:951–64.
27. Israelson A, Zaid H, Abu-Hamad S, et al. Mapping the ruthenium red-binding site of the voltage-dependent anion channel-1. Cell Calcium 2008;43:196–204.
28. Heslop KA, Burger P, Kappler C, et al. Small molecules targeting the NADH-binding pocket of VDAC modulate mitochondrial metabolism in hepatocarcinoma cells. Biomed Pharmacother 2022;150:112928.
29. Ben-Hail D, Begas-Shvartz R, Shalev M, et al. Novel compounds targeting the mitochondrial protein VDAC1 inhibit apoptosis and protect against mitochondrial dysfunction. J Biol Chem 2016;291:24986–5003.
30. Zhang E, Mohammed Al-Amily I, Mohammed S, et al. Preserving insulin secretion in diabetes by inhibiting VDAC1 overexpression and surface translocation in β cells. Cell Metabol 2019;29:64–77.e6.
31. Kim J, Gupta R, Blanco LP, et al. VDAC oligomers form mitochondrial pores to release mtDNA fragments and promote lupus-like disease. Science 2019;366:1531–6.
32. Verma A, Pittala S, Alhozeel B, et al. The role of the mitochondrial protein VDAC1 in inflammatory bowel disease: a potential therapeutic target. Mol Ther 2022;30:726–44.
33. Li Q, Qiao P, Chen X, et al. Affinity chromatographic methodologies based on immobilized voltage dependent anion channel isoform 1 and application in protein-ligand interaction analysis and bioactive compounds screening from traditional medicine. J Chromatogr A 2017;1495:31–45.
34. Rimmerman N, Ben-Hail D, Porat Z, et al. Direct modulation of the outer mitochondrial membrane channel, voltage-dependent anion channel 1 (VDAC1) by cannabidiol: a novel mechanism for cannabinoid-induced cell death. Cell Death Dis 2013;4:e949.

35. Head SA, Shi W, Zhao L, et al. Antifungal drug itraconazole targets VDAC1 to modulate the AMPK/mTOR signaling axis in endothelial cells. Proc Natl Acad Sci 2015;112:E7276–85.
36. Clémençon B, Fine M, Hediger MA. Conservation of the oligomeric state of native VDAC1 in detergent micelles. Biochimie 2016;127:163–72.
37. Yagoda N, von Rechenberg M, Zaganjor E, et al. RAS–RAF–MEK-dependent oxidative cell death involving voltage-dependent anion channels. Nature 2007;447:865–9.
38. Böhm R, Amodeo GF, Murlidaran S, et al. The structural basis for low conductance in the membrane protein VDAC upon β-NADH binding and voltage gating. Structure (London, England: 1993). 2020;28:206–14.e4.
39. Silvers R, Eddy M. NMR spectroscopic studies of ion channels in lipid bilayers: sample preparation strategies exemplified by the voltage dependent anion channel. Methods Mol Biol 2021;2302:201–17.
40. Magrì A, Reina S, De Pinto V. VDAC1 as pharmacological target in cancer and neurodegeneration: focus on its role in apoptosis. Front Chem 2018;6:108.
41. Olivas-Aguirre M, Torres-López L, Pottosin I, Dobrovinskaya O. Phenolic compounds cannabidiol, curcumin and quercetin cause mitochondrial dysfunction and suppress acute lymphoblastic leukemia cells. Int J Mol Sci 2020;22:204.
42. Weiser BP, Bu W, Wong D, Eckenhoff RG. Sites and functional consequence of VDAC-alkylphenol anesthetic interactions. FEBS Lett 2014;588:4398–403.
43. Weber JJ, Clemensson LE, Schiöth HB, Nguyen HP. Olesoxime in neurodegenerative diseases: Scrutinising a promising drug candidate. Biochem Pharmacol 2019;168:305–18.
44. Pinto VD, Al Jamal JA, Palmieri F. Location of the dicyclohexylcarbodiimide-reactive glutamate residue in the bovine heart mitochondrial porin. J Biol Chem 1993;268:12977–82.
45. Hill AP, Sitsapesan R. DIDS modifies the conductance, gating, and inactivation mechanisms of the cardiac ryanodine receptor. Biophys J 2002;82:3037–47.
46. Villinger S, Briones R, Giller K, et al. Functional dynamics in the voltage-dependent anion channel. Proc Natl Acad Sci 2010;107:22546–51.
47. Zaid H, Abu-Hamad S, Israelson A, et al. The voltage-dependent anion channel-1 modulates apoptotic cell death. Cell Death & Differ 2005;12:751–60.
48. Shoshan-Barmatz V, Hadad N, Feng W, et al. VDAC/porin is present in sarcoplasmic reticulum from skeletal muscle. FEBS Lett 1996;386:205–10.
49. Ben-Hail D, Shoshan-Barmatz V. VDAC1-interacting anion transport inhibitors inhibit VDAC1 oligomerization and apoptosis. Biochim Biophys Acta (BBA) - Mol Cell Res 2016;1863:1612–23.
50. Thinnes FP. Does fluoxetine (Prozak) block mitochondrial permeability transition by blocking VDAC as part of permeability transition pores? Mol Genet Metabol 2005;84:378.
51. Nahon E, Israelson A, Abu-Hamad S, Shoshan-Barmatz V. Fluoxetine (Prozac) interaction with the mitochondrial voltage-dependent anion channel and protection against apoptotic cell death. FEBS Letters 2005;579:5105–10.
52. Zizi M, Forte M, Blachly-Dyson E, Colombini M. NADH regulates the gating of VDAC, the mitochondrial outer membrane channel. J Biol Chem 1994;269:1614–6.
53. Rovini A, Gurnev PA, Beilina A, et al. Molecular mechanism of olesoxime-mediated neuroprotection through targeting α-synuclein interaction with mitochondrial VDAC. Cell Mol Life Sci CMLS 2020;77:3611–26.
54. Weiser BP, Kelz MB, Eckenhoff RG. *In vivo* activation of azipropofol prolongs anesthesia and reveals synaptic targets. J Biol Chem 2013;288:1279–85.
55. Malik C, Ghosh S. Quinidine partially blocks mitochondrial voltage-dependent anion channel (VDAC). Eur Biophys J 2020;49:193–205.
56. Murai M, Okuda A, Yamamoto T, et al. Synthetic ubiquinones specifically bind to mitochondrial voltage-dependent anion channel 1 (VDAC1) in *Saccharomyces cerevisiae* mitochondria. Biochemistry 2017;56:570–81.
57. Yang H-L, Tsai C-H, Shrestha S, et al. Coenzyme Q0, a novel quinone derivative of Antrodia camphorata, induces ROS-mediated cytotoxic autophagy and apoptosis against human glioblastoma cells in vitro and in vivo. Food Chem Toxicol 2021;155:112384.
58. Real-Hohn A, Groznica M, Löffler N, et al. nanoDSF: In vitro label-free method to monitor picornavirus uncoating and test compounds affecting particle stability. Front Microbiol 2020;11:1442.
59. Kim SH, Yoo HJ, Park EJ, Na DH. Nano differential scanning fluorimetry-based thermal stability screening and optimal buffer selection for immunoglobulin G. Pharmaceuticals 2021;15:29.
60. Queralt-Martín M, Bergdoll L, Teijido O, et al. A lower affinity to cytosolic proteins reveals VDAC3 isoform-specific role in mitochondrial biology. J General Physiol 2020;152:e201912501.
61. Wienken CJ, Baaske P, Rothbauer U, et al. Protein-binding assays in biological liquids using microscale thermophoresis. Nat Commun 2010;1:100.
62. Shoshan-Barmatz V, Shteinfer-Kuzmine A, Verma A. VDAC1 at the intersection of cell metabolism, apoptosis, and diseases. Biomolecules 2020;10:1485. https://www.ncbi.nlm.nih.gov/pmc/articles/PMC7693975/ [accessed 4 Jan 2021]
63. Puhl AC, Lane TR, Vignaux PA, et al. Computational approaches to identify molecules binding to *Mycobacterium tuberculosis* KasA. ACS Omega 2020;5:29935–42.
64. Solioz M. Dicyclohexylcarbodiimide as a probe for proton translocating enzymes. Trends Biochem Sci 1984;9:309–12.
65. Horn JR, Shoichet BK. Allosteric inhibition through core disruption. J Mol Biol 2004;336:1283–91.